Microstructure of Ag-Sn-Cu-Bi-Ni alloy after oxidation

WU Chun-ping(吴春萍)[1], YI Dan-qing(易丹青)[1], LI Jian(李荐)[1],
WANG Bin(王斌)[1]，XU Can-hui(许灿辉)[1]，LU Xiao-dong(卢小东)[2]

1.School of Materials Science and Engineering, Central South University, Changsha 410083,China；
2.Foshan Electrical Precision Alloy Co. Ltd, Foshan 528000, China

Abstract: Ag-Sn-Cu-Bi-Ni alloy was internally oxidized in air. The phase constitution, surface morphology and microstructure evolution of the alloy after internal oxidation were analyzed by X-ray diffractometry, optical microscopy and scanning electron microscopy, respectively. The results show that the surface color of samples after internal oxidation is different from the different oxidation time and temperatures. The oxidation reaction firstly takes place on the grain boundaries. The microstructure developed on the initial stage of internal oxidation is fir-tree crystal texture. However, this texture structure disappears accompanied by grain growth and oxides forming during the prolonged oxidation. Finally, the oxide particles are uniformly dispersed in the silver matrix.

Key words: Ag-Sn-Cu-Bi-Ni alloy; surface morphology; microstructure; internal oxidation

1 Introduction

The Ag-Cd groups of contact alloys are widely used in tonnages quantities in electrical and electronic industries because of high electrical and thermal conductivities, high resistance to arcing, high welding adhesion resistance, low contact resistance, high hardness and strength[1−4]. However, two European Confederation instructions, ROHS 2002/95/EC and WEEE 2002/96/EC, began execution since June 1, 2006, restrict rigidly the utilization of Cd. This means the European Confederation has completely forbidden the utilization of silver cadmium oxide (Ag-CdO) electrical contact materials[5]. Many investigators have worked on the alternative systems to replace Ag-CdO[6−13].

As the replaced materials of Ag-CdO, the development of Ag-SnO$_2$ materials have gained a great achievement, it has been used widely in business in European Confederation and Japan[14−19]. The method of fabrication Ag-SnO$_2$ materials mainly has powder metallurgy (PM) and internal oxidation (IO) at present. Ag-SnO$_2$ contact materials fabricated by IO method have high resistance to arcing, high welding adhesion resistance, high hardness and strength. But the oxidation of Ag-Sn alloy is difficult when the content of Sn exceed 6%(mass fraction) in silver alloy. In order to enhance the oxidation rate of Ag-Sn alloy, we add Cu and Bi to Ag-Sn alloy. Consequently, the objective of this paper is to investigate microstructure of Ag-Sn-Cu–Bi-Ni alloy after internal oxidation.

2 Experimental

2.1 Materials

Ingots of high purity silver (99.99%) and tin, copper, bismuth, nickel (99.9%) were used to prepare Ag-Sn-Cu-Bi-Ni alloy samples.

2.2 Melting, casting and internal oxidation

Ingots were melted in a medium-frequency induction furnace using graphite crucible. The melt was poured into a preheated square steel mould in the temperature range of 1 100−1 200 ℃ and chilled in air. The square alloy ingot was cut into sizes of 6 mm×6 mm× 6 mm for internal oxidation. The cubic samples were cleaned thoroughly in acetone, alcohol and water to remove surface contaminations for further study.

Internal oxidation experiments were carried out in air at 600 ℃ and 700 ℃ in a muffle furnace.

2.3 Characterization

The phase constitution was analyzed by X-ray diffractometry (D/max2500). And microstructure was characterized by optical microscopy (POLYVAR-MET), scanning electron microscopy (Sirion200 and KYKY2800) and the composition was analyzed by energy spectrometry (Gensis60).

3 Results and discussion

3.1 XRD analysis of samples before and after internal oxidation

XRD spectra of Ag-Sn-Cu-Bi-Ni alloy before and after internal oxidation are shown in Fig.1. Typical peaks of Ag crystals can be detected in the XRD patterns, and the diffraction peak of Sn, Cu, Bi and Ni cannot be detected. In addition, the diffraction peak of Ag becomes broad and takes place deviation. It indicates that Sn, Cu, Bi and Ni atoms have dissolved in Ag crystals and exist in the form of Ag solid solution alloy. The major phase in internal oxidation samples are Ag, SnO_2 and CuO with no indication of Bi_2O_3 and NiO. According to the oxidation character of Bi and Ni, diffraction peaks of Bi_2O_3 and NiO can be detected in the XRD patterns. We can assume that Bi_2O_3 has dissolved in Ag matrix and exist in the form of Bi_2O_3 atomic group. NiO content is too low to be detected in the XRD patterns. As a result, the major phase constitution of Ag-Sn-Cu-Bi-Ni alloy after internal oxidation is Ag, SnO_2 and CuO.
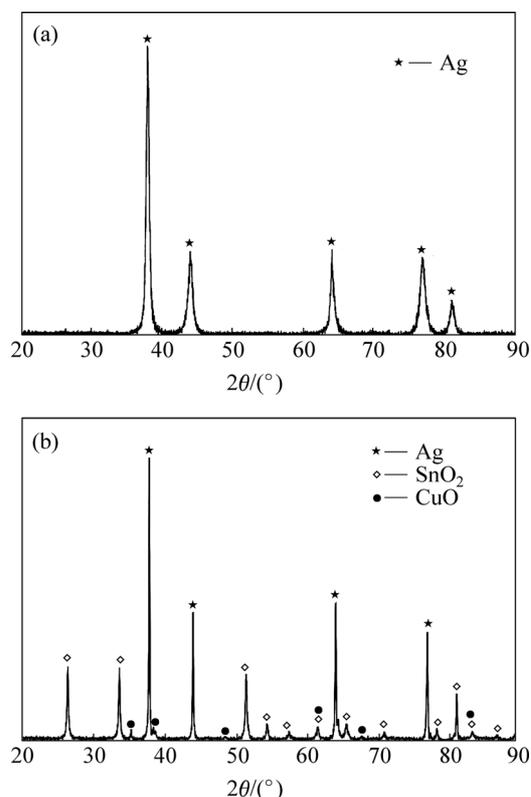

Fig.1 XRD spectra of Ag-Sn-Cu-Bi-Ni alloy: (a) Before internal oxidation; (b) After internal oxidation

3.2 Microstructure characterization of samples

Optical and SEM microstructure of Ag-Sn-Cu-Bi-Ni casting alloy are shown in Fig.2. From Fig.2, we see that the interdendritic distance and segregation are small, indicating that the distribution of Sn, Cu, Bi and Ni in the entitled sample is homogeneous and composition uniformity has been achieved. Fir-tree crystal texture in the materials' microstructure is helpful to internally oxidize because they have a large amount of grain boundary which are helpful to oxygen diffusion in the alloy.
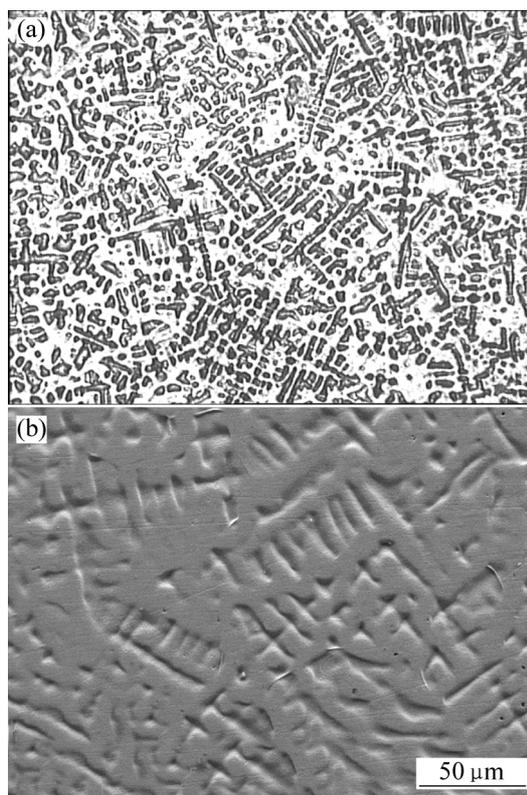

Fig.2 Microstructures of Ag-Sn-Cu-Bi-Ni casting alloy: (a) Optical image; (b) SEM image

3.3 Macromorphology of samples after internal oxidation

The macromorphology of samples after internal oxidation with different time and temperature is shown in Fig.3. From Fig.3, we can see that the surface color of samples is different with the different oxidation time and temperature. At the same oxidation temperature, the surface color of samples becomes gradually light from the fuscous with the oxidation time increase. When the oxidation time is same, the surface color of samples is obviously different with different oxidation temperature. The surface color of samples oxidized at 600 ℃ is dark, but it is gray at 700 ℃.
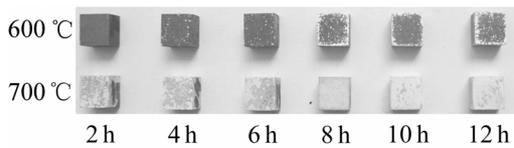
Fig.3 Macromorphologies of samples after internal oxidation with different time and temperatures

3.4 Surface morphology of samples after internal oxidation

The surface morphologies of samples after internal oxidation in air at 600 ℃ for different holding time are shown in Fig.4. It can be seen from Fig.4 that the surface morphologies are different with different holding time. As shown in Fig.4(a), large majority of the oxides take spherical shape. Oxidation at air assures adequate oxygen diffusion on the initial stage of internal oxidation. Consequently, oxides grow uniformly along all directions and form spherical particles. However, there are different surface morphologies in Figs.4(b)−(f), where two kinds of oxides are observed in the silver matrix. Oxide particles with diameter below 1 μm are uniformly dispersed inside the grains (for instance region A), those flake oxides are presented on grain boundaries (for instance region B). EDS result of region A and B are shown in Fig.5(a) and (b) respectively. From Fig.5(a) and (b), we can see that the flakes on the grain boundaries and the particles in the grain are oxides. In addition, the content of oxides on the grain boundaries is higher than that in the gain. It indicates that the oxidation reaction firstly takes place on the grain boundaries. Since the defect concentration of grain boundaries are higher than that in grains, the oxygen firstly diffuses into the grain boundaries and takes place oxidation reaction with alloy agent. With increasing oxidation temperature and time, the oxygen will diffuse into grain interior and react with metal elements. As a result, the oxides on the grain boundaries are more than that in grains.
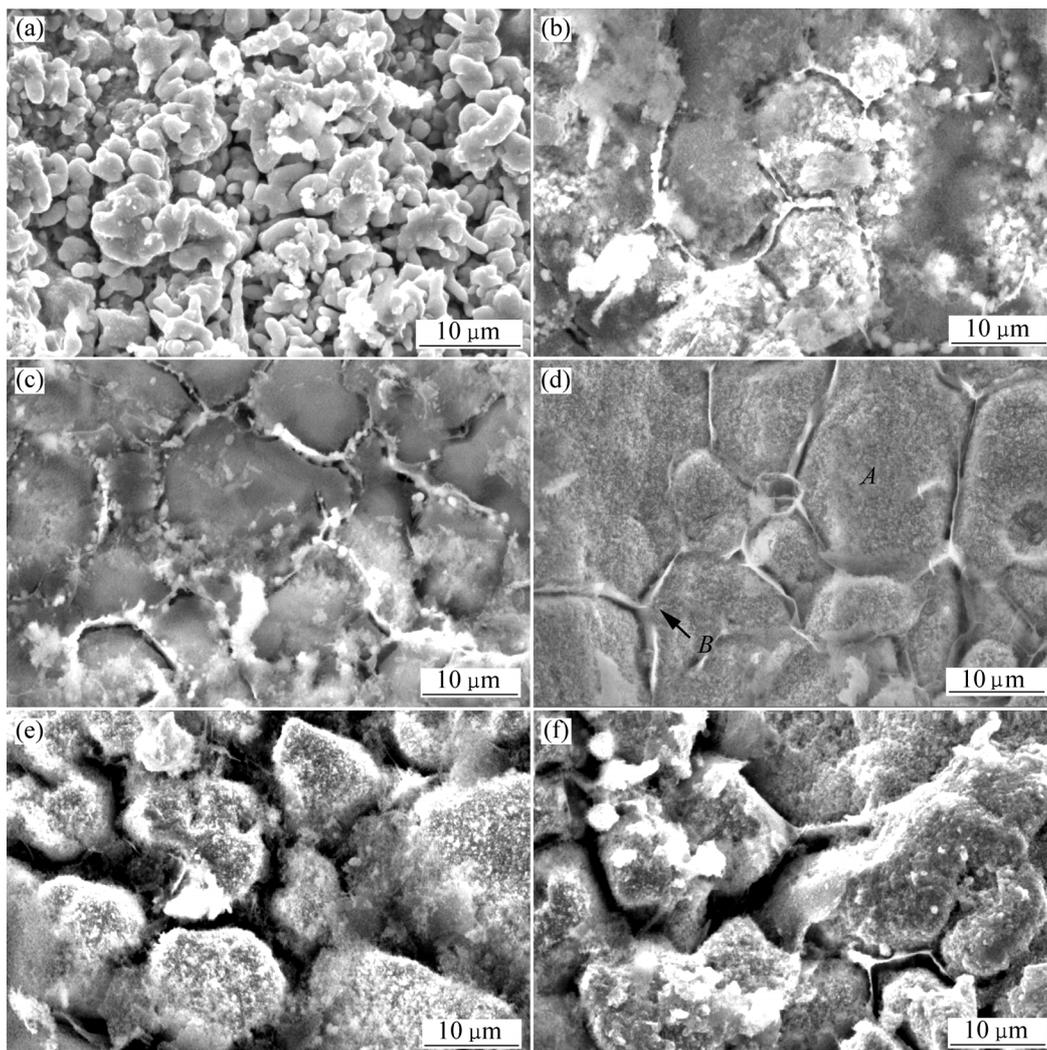

Fig.4 Surface morphologies of samples after internal oxidation for different time: (a) 12 h; (b) 24 h; (c) 36 h; (d) 48 h; (e) 60 h; (f) 72 h
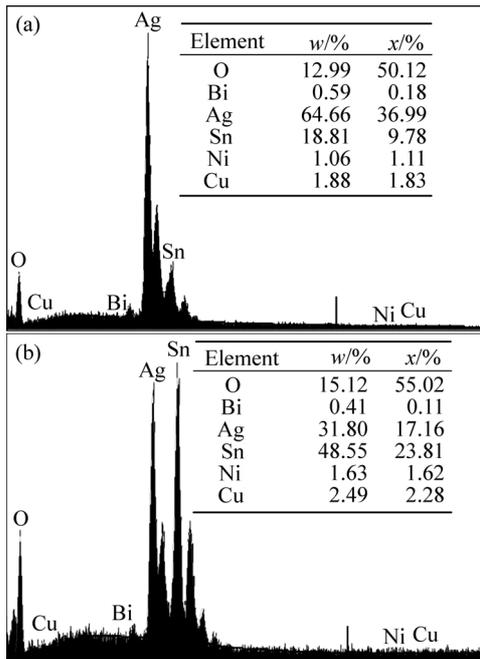
Element	w/%	x/%
O	12.99	50.12
Bi	0.59	0.18
Ag	64.66	36.99
Sn	18.81	9.78
Ni	1.06	1.11
Cu	1.88	1.83

Element	w/%	x/%
O	15.12	55.02
Bi	0.41	0.11
Ag	31.80	17.16
Sn	48.55	23.81
Ni	1.63	1.62
Cu	2.49	2.28

Fig.5 EDS results of region A(a) and region B(b) shown in Fig.4

3.5 Optical microstructures of samples after internal oxidation

Optical microstructures of Ag-Sn-Cu-Bi-Ni alloy samples after internal oxidation in air at 600 ℃ for different holding time are shown in Fig.6. From Fig.6 we can find that the microstructure is changed after internal oxidation. On the initial stage (holding for 2 h and 4 h) of internal oxidation the microstructure is still fir-tree crystal texture (see Figs.6(a) and Fig.6(b)), where the interdendritic distance is larger than that in Fig.3. However, the fir-tree crystal texture has disappeared accompanied by grain growth and oxides formation during the prolonged oxidation (see Figs.6(c)− (f)). From Figs.6(c)−(f) we can see that the oxide particles uniformly disperse in the silver matrix. The oxide particles uniformly dispersing in the silver matrix can strengthen the silver alloy. As a result, the internally oxidized silver alloy have high resistance to arcing and welding.
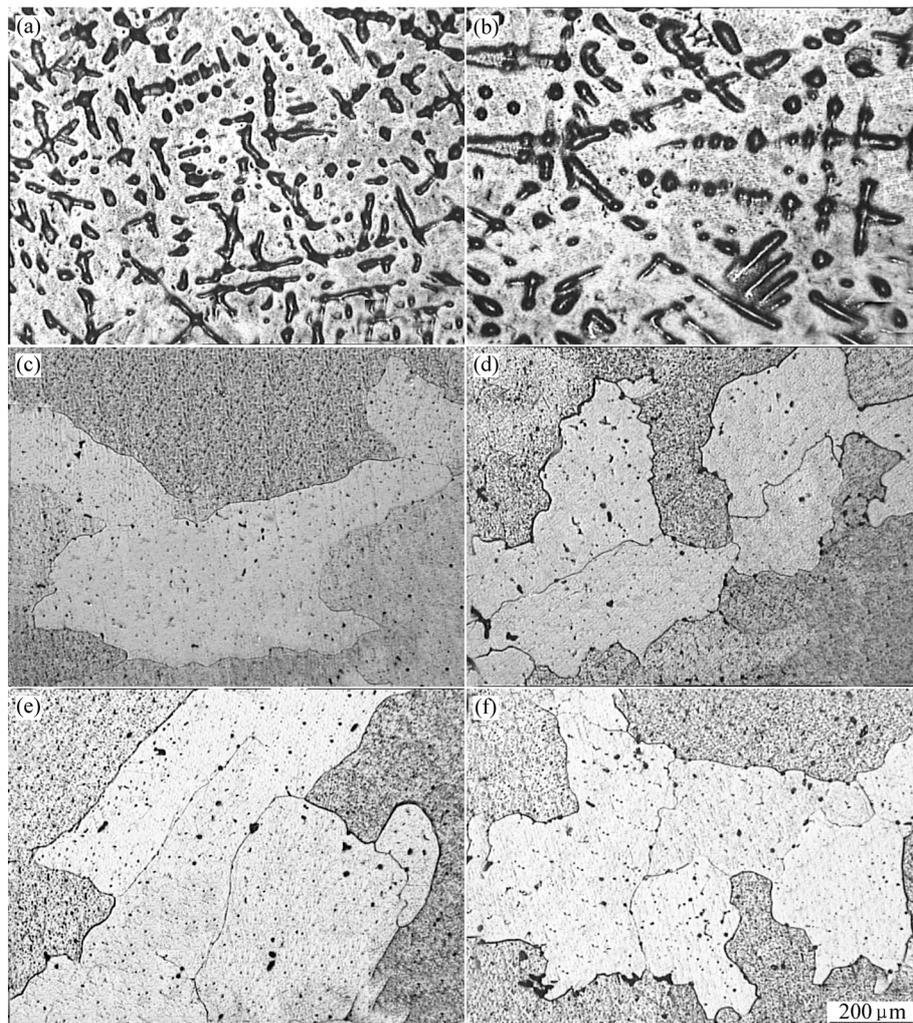

Fig.6 Optical microstructures of Ag-Sn-Cu-Bi-Ni alloy samples after internal oxidation for different time: (a) 2 h; (b) 4 h; (c) 6 h; (d) 8 h; (e) 10 h; (f) 12 h

4 Conclusions

1) The major phase constitution of Ag-Sn-Cu-Bi-Ni alloy after internal oxidation is Ag, SnO_2 and CuO, whereas Bi_2O_3 has dissolved in Ag matrix and exists in the form of Bi_2O_3 atomic group.

2) The surface color of Ag-Sn-Cu-Bi-Ni alloy is different with the different oxidation time and temperature. At the same oxidation temperature, the surface color of samples becomes gradually light from the fuscous with the oxidation time increase. The surface color of samples oxidized at 600 ℃ is dark, but it is gray at 700 ℃.

3) The oxidation reaction firstly takes place on the grain boundaries. The microstructure developed on the initial stage of internal oxidation is fir-tree crystal texture. However, this texture structure lately disappears accompanied by grain growth and oxides forming during the prolonged oxidation. Finally, the oxide particles are uniformly dispersed in the silver matrix.

References

[1]   RONG Ming-zhe, WANG Qi-ping. Surface dynamics and it's reaction to the effect of breaking arc for AgMeO contact[C]// Proc of 16th ICEC. Loughborough, 1992: 389−394.

[2]   SAWA K, HASEGAWA M. Recent researchers and new trends of electrical contacts[J]. IEICE Trans on Electric, 2000, 83(9): 1363−1376.

[3]   MANHAET H. Arc mobility on new and eroded AgCdO and AgSnO₂ contacts[J]. IEEE CHMT, 1989, 12(1): 48−57.

[4]   BRECHER C, GUSTAFSON J. The effect of additive concentration on material erosion matrix-strengthened silver-cadmium oxide[J]. IEEE Trans Components, Hybirds, Manuf, Technol, 1984, 7(1): 91−96.

[5]   CHEN Jing-chao, SUN Jia-lin, DU Yan. The limiting policy of silver cadmium oxide and the development of the other silver metal oxide electrical contact materials[J]. Electric Engineering Materials, 2002(4): 41−44. (in Chinese)

[6]   SHUBATA A. Silver/metal oxide contact material by internal oxidation process[C]// Proc 7, ICEC. Pairs, 1974: 749−754.

[7]   WEI Juan. Sliver cadmium oxide electrical contact material and its development[J]. Nonferrous Metal, 1992(4): 68−73. (in Chinese)

[8]   ZHANG Wan-sheng. The overseas basic situation of electrical contacts[J]. Electrical Alloy, 1995(1): 1−14. (in Chinese)

[9]   CHEN Li-cao, LI Zhong-bin. The optimizing problem of Ag/SnO₂ contact materials for contactors[J]. Electrical Alloy, 1993(4): 1−5. (in Chinese)

[10]   BEHREN N, BOHM W. Switching performance of different Ag/SnO₂ contact materials made by powder metallurgy[C]// 11th ICEC. Berlin, 1982: 203−209.

[11]   BRAUMANN P, KOLB H, WEISE W. Optimization of Ag/SnO₂ contact material for use in contactors[J]. 16th ICEC. Loughborough, 1992: 163−168.

[12]   ZHANG Guo-qing, DENG De-guo, QI Geng-xin, GUO Jun-mei, GUAN Wei-ming. The analysis of the deformation fracture of Ag/SnO₂ composite materials[J]. Noble Metal, 1999, 20(4): 1−6. (in Chinese)

[13]   ZHANG Qi-sun, XIE Jian-qiu. Silver copper oxide contact material of powder metallurgy[J]. The Chinese Journal of Nonferrous Metals, 1996, 6(2): 121−124. (in Chinese)

[14]   BEHERNS N, BOHM W. Switching performance of different AgSnO₂ contact materials made by powder metallurgy[C]// Lectures of the 11th International Conference on Electrical Contact Phenomena. Berlin, 1984: 203−220.

[15]   BRAUMANN P, KOLB H, SCHRODER K. H,WEISE W. Optimization of Ag/SnO₂ contact material for use in contactors[C]// Proceedings of the 16th International Conference of Electrical Contacts. Loughborough, 1992: 163−168.

[16]   BOURDA C, JEANNOT D, PINARD J, RANONI P. Properties and effects of doping agents used in AgSnO₂ contact materials[C]// Proceedings of the 16th International Conference of Electrical Contacts. Loughborough, 1992: 377−382.

[17]   BEHRENS V, HONIG TH, KRAUS A, MICHALl R, MINKENBERG N, SAEGER K E. Ag/SnO₂ WPX a new type of silver /tin oxide contact materials[C]// Proceedings of the 17th International Conference of Electrical Contacts. Nagoya, 1994: 613−618.

[18]   CHEN Jing-chao, SUN Jia-lin, ZHANG Kun-hua. Silver tin oxide electrical contact material fabricated by reactive synthesis[C]// ICEC. Zurich, 2002: 447−451.

[19]   LIU X M, WU S L, PAULl K. Effects of coating process on the characteristics of Ag/SnO₂ contact materials[J]. Materials Chemistry and Physics, 2006(98): 477−480.

(Edited by YANG Hua)